remote sensing

MDPI

Article

Advanced Three-Dimensional Finite Element Modeling of a Slow Landslide through the Exploitation of DInSAR Measurements and in Situ Surveys

Vincenzo De Novellis [1], Raffaele Castaldo [1], Piernicola Lollino [2], Michele Manunta [1] and Pietro Tizzani [1,*]

[1] Istituto per il Rilevamento Elettromagnetico dell'Ambiente, IREA-CNR, via Diocleziano 328, 80124 Napoli, Italy; denovellis.v@irea.cnr.it (V.D.N.); castaldo.r@irea.cnr.it (R.C.); manunta.m@irea.cnr.it (M.M.)

[2] Istituto di Ricerca per la Protezione Idrogeologica, IRPI-CNR, via Amendola 122 I, 70126 Bari, Italy; p.lollino@ba.irpi.cnr.it

* Correspondence: tizzani.p@irea.cnr.it; Tel.: +39-081-7620635

Academic Editors: Roberto Tomas, Zhenhong Li, Richard Gloaguen and Prasad S. Thenkabail
Received: 10 June 2016; Accepted: 16 August 2016; Published: 19 August 2016

Abstract: In this paper, we propose an advanced methodology to perform three-dimensional (3D) Finite Element (FE) modeling to investigate the kinematical evolution of a slow landslide phenomenon. Our approach benefits from the effective integration of the available geological, geotechnical and satellite datasets to perform an accurate simulation of the landslide process. More specifically, we fully exploit the capability of the advanced Differential Synthetic Aperture Radar Interferometry (DInSAR) technique referred to as the Small BAseline Subset (SBAS) approach to provide spatially dense surface displacement information. Subsequently, we analyze the physical behavior characterizing the observed landslide phenomenon by means of an inverse analysis based on an optimization procedure. We focus on the Ivancich landslide phenomenon, which affects a residential area outside the historical center of the town of Assisi (Central Italy). Thanks to the large amount of available information, we have selected this area as a representative case study highlighting the capability of advanced 3D FE modeling to perform effective risk analyses of slow landslide processes and accurate urban development planning. In particular, the FE modeling is constrained by using the data from 7 litho-stratigraphic cross-sections and 62 stratigraphic boreholes; and the optimization procedure is carried out using the SBAS-DInSAR retrieved results by processing 39 SAR images collected by the Cosmo-SkyMed (CSK) constellation in the 2009–2012 time span. The achieved results allow us to explore the spatial and temporal evolution of the slow-moving phenomenon and via comparison with the geomorphological data, to derive a synoptic view of the kinematical activity of the urban area affected by the Ivancich landslide.

Keywords: 3D Finite Element model; landslides kinematics; Cosmo-SkyMed DInSAR measurements; Ivancich landslide (Assisi, Central Italy)

1. Introduction

The assessment of the kinematical evolution of the slow landslides is challenging for the analysis and zonation of the risk in urban areas. Indeed, the capability to detect the spatial kinematical variability of a slow landslide processes can represent a fundamental source of knowledge to support the land management decision for the development of infrastructures in urban areas. In this perspective, the evaluation of the landslide displacement field at ground level in a certain time span, can impart

important information for the prediction of the expected damage to buildings and infrastructure. In addition, the understanding of the landslides kinematics is also crucial in defining efficient prevention and mitigation strategies and can be effectively pursued only if multidisciplinary data, both in terms of temporal and spatial coverage of the area is available.

The kinematics of the landslide phenomena has been analyzed in a large number of scientific studies; the approaches range from the analytical one-dimensional (1D) infinite slope models, suitable for landslides bodies with sliding surface depth about constant and significantly lower than the landslide length [1–5], to more sophisticated two- (2D) and three-dimensional (3D) Finite Element (FE) models aimed at detecting the different kinematical sectors along the slope area [6–9]. In particular, the recent development of three-dimensional numerical codes allows us to carry out simulations of the displacement rate field of a landslide process in a more realistic and accurate way. The simulations of the landslide kinematics are achieved through the implementation in a numerical domain, of the available a-priori information on the slope, as the topography, the landslide body geometry and the mechanical properties of the involved geomaterials. Such enhanced information is retrieved through a significant increase of the computational load of the 3D models with respect to 2D models. However, this computational complexity can be correctly reduced when the examined landslide shows the typical kinematical features of a landslide creep, i.e., landslide phenomena are characterized by very low pore water pressure variation rates and consequently, the displacement rates do not significantly change with time.

The reliability of the performed numerical models significantly improves when the same models are calibrated and validated by using the measurements collected by means of the available monitoring networks. To this purpose, the inverse analysis carried out via optimization procedures aimed at searching for the model best-fitting solution against the monitoring dataset, represents a very efficient tool in identifying the physical process that governs the observed phenomenon [8,9]. To accomplish an effective inverse analysis of a 3D landslide model, spatially distributed surface measurements are needed. In particular, a network of displacement measure points that covers a large portion of the landslide body is required to correctly constrain the three-dimensional FE model. However, surface deformation measurements based on in situ research (inclinometers, GPS, leveling) are often unavailable, or only partially available, due to the high costs related to these technologies, especially if needed for long-term research. In this context, satellite techniques offer an effective and reliable alternative or a complementary tool to traditional in situ research. In particular, the Differential Synthetic Aperture Radar (SAR) Interferometry (DInSAR) techniques are becoming a powerful tool for monitoring, with centimeter to millimeter accuracy, the spatial and temporal evolution of slow deformation phenomena [10]. In the last few years, the DInSAR technique has been used to detect, study and monitor the surface displacements related to mass movement and slope instabilities [11–13] through the availability of several advanced DInSAR algorithms able to retrieve deformation time series and velocity maps [14–17]. Among the DInSAR techniques currently available, the Small BAseline Subset (SBAS) approach [16,17] has well demonstrated its capability in monitoring the deformations related to mass movement phenomena with high spatial density of measure points [18]. The SBAS DInSAR measurements have already used the implement optimization procedure for the FE model of a landslide process, mainly in two-dimensional domains [8]. Although the proposed studies have allowed us to deeply explore the landslide kinematics along the considered 2D section, the achieved results do not permit us to fully clarify the role of the geometrical and geological three-dimensional features in the distribution of the deformation field at ground surface.

The present work (the Ivancich landslide, which affects a residential area outside the historical center of the Assisi town, Central Italy), has been selected as a representative case study to highlight the capability of advanced three-dimensional FE modeling as a complementary tool in performing an effective risk analyses of the slow landslide processes and accurate urban development planning (Figure 1).

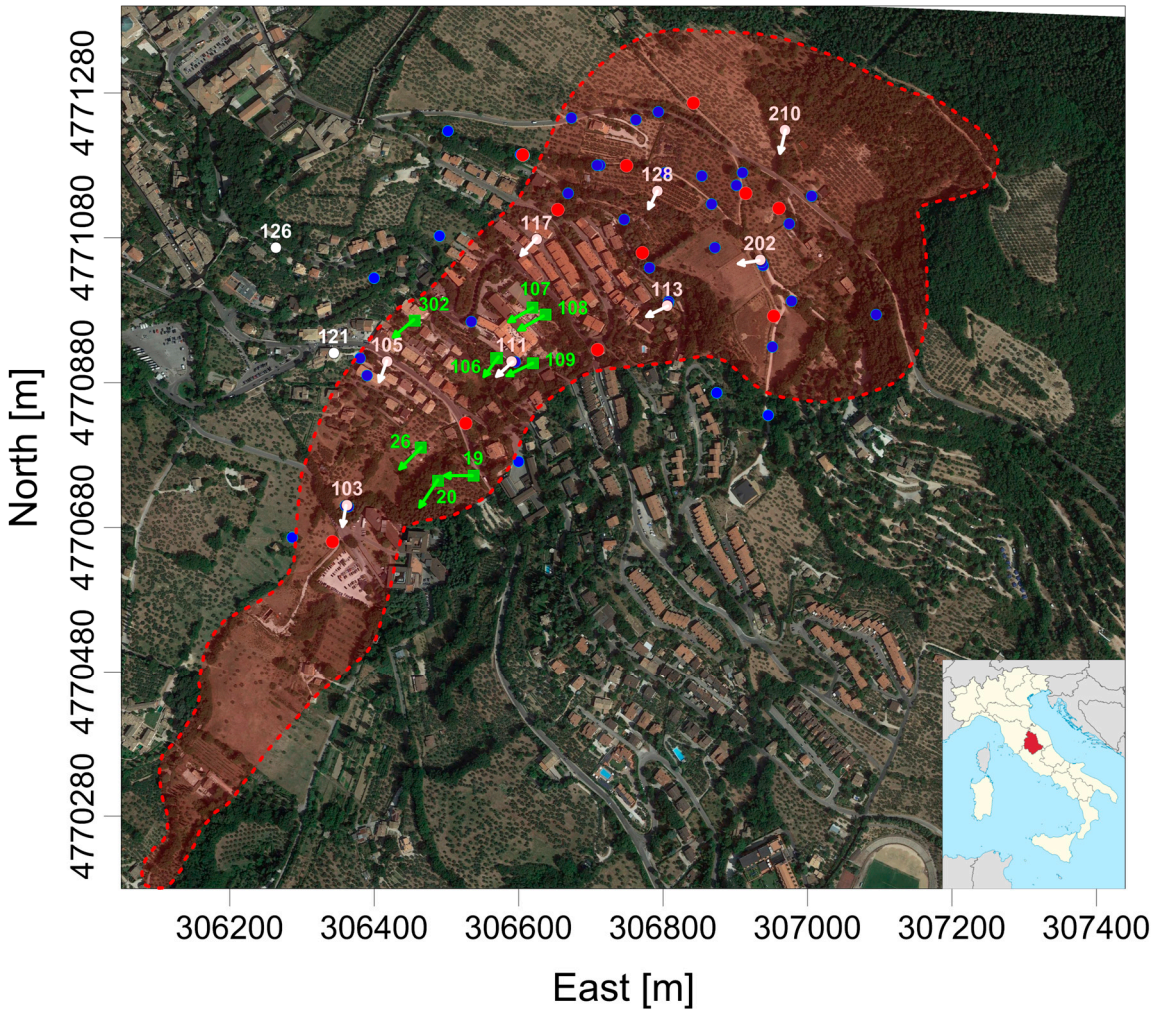

Figure 1. Study Area. Satellite optical image (source: Google Earth) of the Assisi surrounding area (Central Italy) affected by the Ivancich landslide. Insert map, lower right corner, reports the geographic location of the study area. Shaded area with red contour shows the zone involved by the recent slope instability phenomenon. All the circles represent borehole data: blue circles represent the 1998 survey; white circles are inclinometric boreholes (related to the same time period of the blue boreholes); red circles correspond to the 2006 survey. The green squares identify the previous inclinometric survey, acquired during 1982–1990 time interval. The arrows indicate the direction of the landslide movement.

The Ivancich landslide is an ancient landslide phenomenon and consists of a slow deep-seated mass movement, which can be classified as a typical earth-slide [19]. Although the rate of movement is very slow, the landslide has caused major damage to buildings, roads and infrastructures due to the effect of accumulation of ground differential displacements over time [20,21]. The first evidence of landslide activity were recorded in 1399 on the ancient Franciscan convent, which represented at that time the only anthropic structure of the area. In accordance with the demographic development that followed the end of World War II, the town of Assisi and its surrounding was intensely urbanized. Consequently around 1970, further evidence of landslide mobility started to appear in the form of growing damage to buildings, retaining walls, pipelines and road paving. The infrastructure damage led local authorities in carrying out several geological and geotechnical investigations aimed at studying the landslide process and designing the mitigation strategies [20,22]. Indeed, the area has been deeply investigated over the last 20 years and extensively monitored through in situ inclinometers, piezometers and GPS measurements [23–25]. At the same time, remote sensing techniques have been

exploited in order to achieve dense spatial information of the unstable mass [18,26]. Such a large availability of measurements and in situ data makes the Ivancich landslide a real-scale laboratory in order to test and validate new approaches and techniques based on the integration of multi-source data. In this scenario, the FE modeling approach, based on the integration of available geological, geotechnical and satellite dataset, is aimed at investigating the 3D kinematical evolution of the landslide in the different sectors of the instability process. In particular, we exploit 39 SAR images collected by the Cosmo-SkyMed (CSK) constellation in the 2009–2012 time period, 7 litho-stratigraphic cross-sections and 62 stratigraphic boreholes.

Finally, the achieved outcomes allow us to investigate the spatial and temporal evolution of the slope affected by slow-moving phenomenon and via comparison with the geomorphological data, to derive insights into the kinematical activity map of the whole area affected by the Ivancich landslide.

2. Measurement Datasets

2.1. Geological and Geomorphological Data

From the 1970s to the present day, the Ivancich landslide has been deeply investigated from a geological and geotechnical point of view, so that the geometry of the active landslide has been quite accurately defined. The landslide morphology is characterized in the upper part by the presence of banks and detachment surfaces; secondary banks and smaller detachment niches are also present inside the landslide body; the lower zone of the landslide has a smaller slope inclination, showing an evident accumulation area with a tongue shape. The landslide has a total length of 1.4×10^3 m from the scarp of the source area to the nail of the toe area and the total surface area is estimated to be about A = 4.1×10^5 m^2 (Figure 1); the slope presents an average inclination of about 21%. In addition, the geomorphological and topographic surveys revealed that the slope movement is an old translational slide, with a rotational component in the source area which moves along a well-defined shear band [18]. In particular the mass movement involves a debris deposit from 15 to 60 m in thickness, overlaying bedrock that consists of a pelitic sandstone unit and layered limestone. The performed in-situ investigations (also from the analysis of 62 stratigraphic boreholes) allow us to reconstruct with a high degree of accuracy, the depth of the bedrock and the geometry of the sliding surface (Figure 1). The unstable mass consists of a debris mass flowing over a stable bedrock composed of marl, sandstone and limestone (Figure 2a). Both transverse and longitudinal litho-stratigraphic sections highlighting the thickness of the landslide debris have been reconstructed (Figure 2b). The bedrock is characterized by a pelitic sandstone formation that consists mainly of marl, clay marl and calcareous marl and sandstone with variable thickness, from a few centimeters to several meters. The shallower part of the bedrock, in contact with the landslide detritus, is strongly weathered. The marl and marly limestone formation is characterized by calcareous marl stratification hardly distinguishable owing to the intense cleavage.

As explained before, the contact with the detritus is represented by a marked alteration band with a thickness not larger than 2 m, which can be recognized as the shear zone delimiting the landslide body. A fundamental constraint for the modeling approach, which is presented later on, derives from electric piezometer cell recordings, which do not measure relevant variations of the pore water pressures at the depth of the shear band. In particular, the ground water surface is measured to be only few meters above the shear band, resulting in very low piezometric heights, when compared to the total stress levels [18]. This further confirms the assumption of a landslide creep.

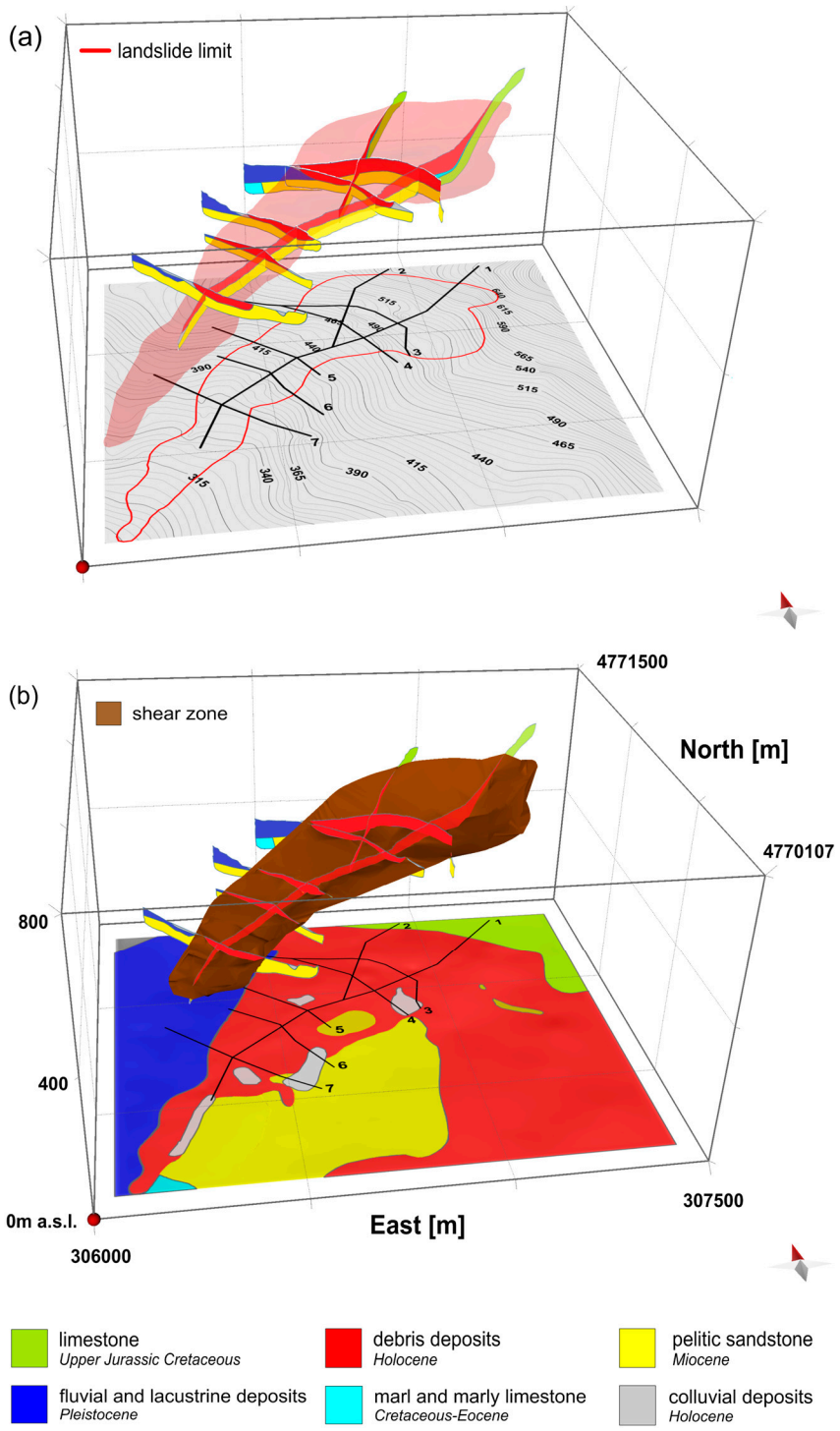

Figure 2. 3D view of geo-lithological data. Cross-sections of Ivancich area and the related traces are reported in the maps of panel (**a**) and (**b**) as black lines; (**a**) Contour of topographic map: the red line and the red shaded area indicate the boundaries and the area of the landslide, respectively; (**b**) Geological map: the brown surface represents the shear zone. In the legend we report the different lithologies of the cross section and geological map.

2.2. Inclinometric Measurements

From 1982 to 2008, numerous investigations of sub-surface landslide area, consisting of borehole inclinometer measurements [14,23], have been carried out in order to define the geometry of the sliding

mass and to acquire data on the sub-surface displacement trend (Figure 1). All inclinometer data, except for n°121 and n°126 (outside the landslide area), indicate an abrupt increment of the cumulated displacements along the vertical profile, at depths ranging between 10 and 55 m, from the top to the toe of the landslide; the spatial correlation of this information has allowed us to identify the depth of the sliding surface throughout the landslide area. Therefore, the measurements acquired between 1998 and 2005, complementary to the satellite monitoring of the landslide kinematics, highlight the existence of a shear zone characterized by a thickness lower than 2 m, over which the landslide debris moves approximately as a rigid body [20].

The n°103 inclinometer shows a cumulated displacement at the ground surface of about 7 cm from January 1999 to October 2009 (displacement rate approximately equal to 0.6 cm/yr); for n°113 inclinometer, the measurements from December 1998 to December 2005 show a cumulated displacement at the ground surface of about 7.5 cm (approximately 1 cm/yr); for n°117 inclinometer, the measurements show a cumulated displacement at the ground surface of 6 cm, from December 1998 to July 2004 (approximately 1 cm/yr). Moreover, at the inclinometers located in the uppermost area of the landslide, slightly lower values of cumulated displacements were recorded: the inclinometers n°128 and n°202 respectively show about 3 cm between March 1999 and December 2008 (average displacement rate = 0.3 cm/yr) and about 4 cm between December 1998 and February 2008 (displacement rate = 0.4 cm/yr). Therefore, the inclinometer data indicate that the major landslide activity involves the central sector. It is worthwhile pointing out that the available inclinometers dataset [20,23,24] is utilized in order to spatially constrain the three-dimensional geometry of the shear-band, which delimits the landslide unstable mass at depth, as already demonstrated by Castaldo et al. [8].

2.3. Satellite Data

To rely on a large network of surface deformation measure points, we also benefit from remote sensing observations. In particular, we use the results achieved by applying the DInSAR technique for monitoring the surface deformations caused by the Ivancich landslide. DInSAR is an active microwave remote sensing technique that exploits the phase difference (i.e., the interferogram) between SAR image pairs acquired over the same area at different times, in order to extract information on the projection along the radar Line Of Sight (LOS) of the surface deformations that occurred between the two SAR acquisitions [27]. Among the several DInSAR techniques, in this work we benefit from the full resolution Small BAseline Subset (SBAS) approach [17,28] that has the capability to retrieve a very large number of measure points by processing only interferograms less affected by noise (small baseline interferograms) [16]. The SBAS DInSAR approach has been successfully applied in analyzing deformation phenomena caused by natural and human-induced processes, resulting a useful tool for the assessment and mitigation of the hydrogeological and urban risk [18,29–33]. Such a capability allows us to map the whole zone covered by the mass movement, by retrieving accurate and spatially dense information on the surface displacements affecting the investigated area.

The Ivancich landslide has been studied by using different SAR datasets to detect surface displacements and to carry out their long-term monitoring [18,26,30]. In this work, we benefit from the images acquired by the Cosmo-SkyMed (CSK) constellation. The CSK system is able to collect a sequence of SAR images of the Earth's surface with very short revisit time (4 days in the interferometric mode) and high spatial resolution (3 m in the stripmap mode and 1 m in the spotlight mode). These characteristics allow us to significantly increase, up to 15 times, the measure point density with respect to ERS-ENVISAT analyses, as demonstrated by Calò et al. [18]. This improvement is particularly significant in investigating the Ivancich landslide by integrating satellite measurements with in situ information since they allow a detailed analysis of the spatial distribution of the ground deformations. The CSK DInSAR measurements (Figure 3) already presented by Calò et al., [18], are retrieved by processing 39 images acquired from descending orbits between December 2009 and February 2012.

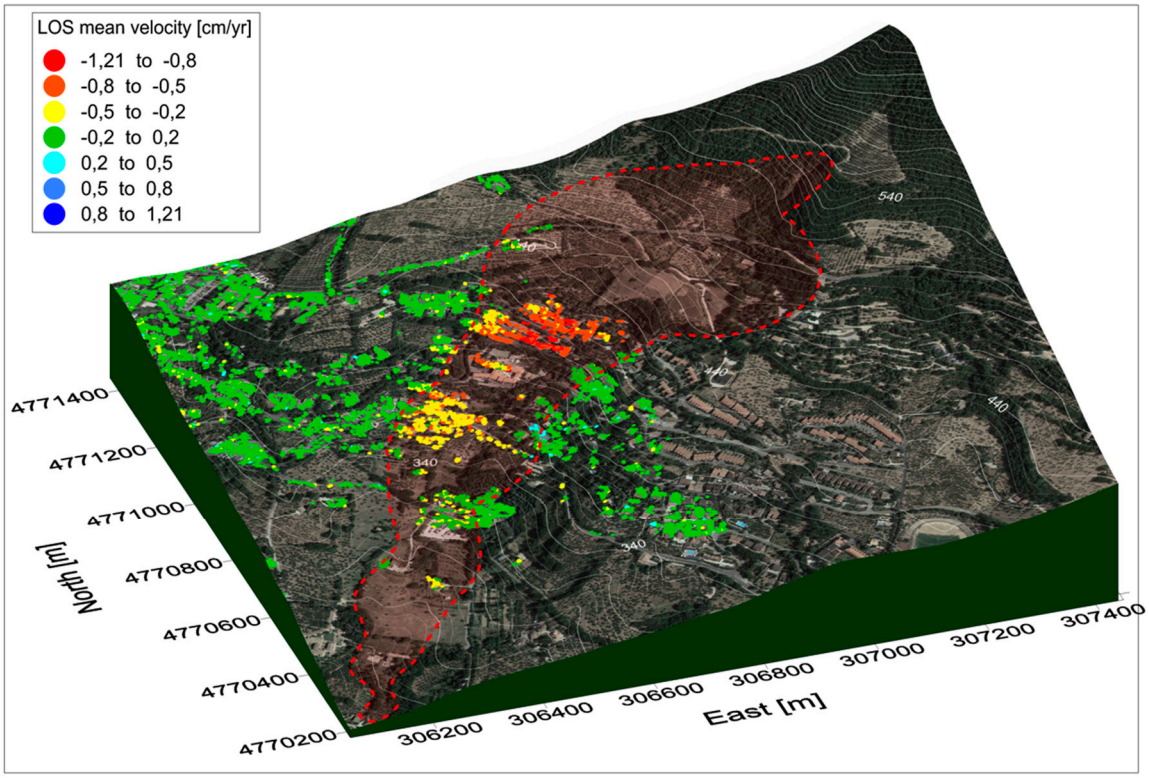

Figure 3. DInSAR measurements. CSK LOS mean deformation velocity map superimposed on the 3D view of satellite optical image with the DEM contour lines (grey lines). The red shade shows the zone involved by the recent instability phenomenon.

According to Bovenga et al., [26], Calò et al., [18] and Castaldo et al., [8], the DInSAR measurements show a quasi-linear LOS displacement trend (Supplementary Materials Figure S1), and a slight increase of the displacements over long time period. Similar outcomes have also been retrieved through the analysis of the measurements provided by a GPS network consisting of 16 stations [25]. Such a study shows that the maximum displacement values are observed in the central part of the landslide body and the vector direction follow the maximum slope line. The deformation trends have been evaluated on a long-term period and confirm a quasi-linear behavior with a value of squared correlation coefficient very close to the unity (R^2 = 0.988) [25].

The kinematic of Ivancich landslide is characterized, in the considered time interval (2009–2012), by a movement of the unstable mass directed downwards following the maximum slope line. The displacement rate is quite slow since the estimated maximum LOS mean velocities are of the order of 1 cm/yr as measured in the middle-upper area of the landslide body; lower displacement rates have been measured both in the lower and in the uppermost area of the landslide. The displacement rate values are in good agreement with those resulting from the inclinometer data (see Section 2.2), showing LOS velocities practically constant over time. As regards to the middle-upper sector of the landslide, Figure 3 also reveals a reduction of the LOS velocities measured for pixels located close to the right-hand side of the landslide body, in the range from −0.2 to −0.5 cm/yr, with respect to those observed in the central portion at corresponding elevations (−0.5 to −1.2 cm/yr). This result indicates a clear spatial variation of the landslide kinematical evolution, with higher velocities along the longitudinal axis and lower values along the lateral boundaries. In addition, the ground displacement velocity field, estimated via interferometric data processing, were in good agreement with the superficial boundaries of the landslide body as derived from the geomorphological analysis (Figure 3). However, this comparison is possible only for the coherent SAR pixels, which are located mainly in the central region of the unstable mass.

Finally, the SBAS-DInSAR displacement time-series also provide additional information regarding the effects of the rainfall regime on the landslide behavior. As a matter of fact, a comparative analysis of the landslide kinematics with the rainfall records for the same period [18] indicate the absence of a direct/immediate response of the surface deformation to the rainfall regime and furthermore, a complex temporal interaction between rainfall amount and ground movements. Accordingly in the advanced FE analysis described in the following section, we consider the possible effects due to rainfall as negligible and approximately assume the soil system as a single-phase material.

3. Three-Dimensional Finite Element Modeling

In this work, we exploit a numerical approach based on an optimized three-dimensional FE model that is constrained by DInSAR and field measurements. In particular, we combine the benefits of a deterministic numerical approach with statistical methods aimed at improving and optimizing the obtained numerical solution in order to analyze and interpret the ground deformations measured in the whole landslide area.

Based on the linearity of kinematics affecting the unstable mass, as observed according to the landslide monitoring dataset, we carry out the three-dimensional FE modeling of the active ground deformation field by assuming, as a first approximation, the soil material behavior as Newtonian fluid characterized by viscosity constant over time. We remark that this model can be applied mainly to landslide cases where the shear zone geometry is well formed and well known by means of accurate and detailed in-situ investigations. In this scenario, the distribution of the soil viscosity parameter within the whole numerical domain can be evaluated through an advanced procedure that implements a nonlinear optimization of the model parameters aimed at simulating the CSK DInSAR measurements. Accordingly, we can assume a steady-state viscous flow (Newtonian fluid) solved through the incompressible Navier–Stokes differential equations:

$$\begin{cases} -\nabla\cdot\,\mu\,(\nabla\boldsymbol{u}\,+(\nabla\boldsymbol{u})^{T})+\rho\,(\boldsymbol{u}\cdot\nabla)\boldsymbol{u}+\nabla\mathrm{p}=\mathbf{F} \\ \nabla\cdot\,\boldsymbol{u}=0 \end{cases} \tag{1}$$

where **u** [m/s] is the deformation velocity vector; **F** [Pa/m] is the body force term; ρ [kg/m^3] is the density; p [Pa] is the pressure; and μ is the dynamic viscosity [Pa·s] (hereafter referred to as viscosity) [34].

The first step of the analysis deals with the setup of the a priori geo-lithological model. The interpretation of the available geological data provides a more accurate insight on the landslide geological conditions, as well as a more effective view capability of complex geological processes. In particular, in a geo-referenced system, the DEM (Digital Elevation Model), the geological map, the lithological cross-sections and the inclinometric borehole data are taken into account (Figure 4a,b) to define a realistic 3D geo-lithological model (1.5 × 1.5 × 0.1 km^3) of the Ivancich area.

Consequently, we have implemented the 3D geo-lithological model of the whole landslide divided into five geo-mechanical units within a numerical environment (see Table 1 for the corresponding physical properties): the limestone bedrock, in the upper part of the slope; the pelitic sandstone bedrock in the central and lower portions of the slope; the landslide deposit formed of unsorted debris; the colluvial deposit in the landslide toe area; the shear zone characterized by thickness of less than 2 m at depths ranging between 15 and 60 m from the ground surface.

The performed 3D geo-lithological model allows us to finely define the geometric features of the shear zone beneath the landslide deposit. Subsequently, we divided the shear zone into three sectors characterized by a homogenous viscosity value (Figure 4b), in accordance with both the geomorphological features along the slope and the kinematical behavior observed for the different portions of the landslide. The evidence of the existence of different landslide kinematical sectors is also supported by the analysis of the DInSAR measurements, which proves that the identified sectors are characterized by different kinematical rates.

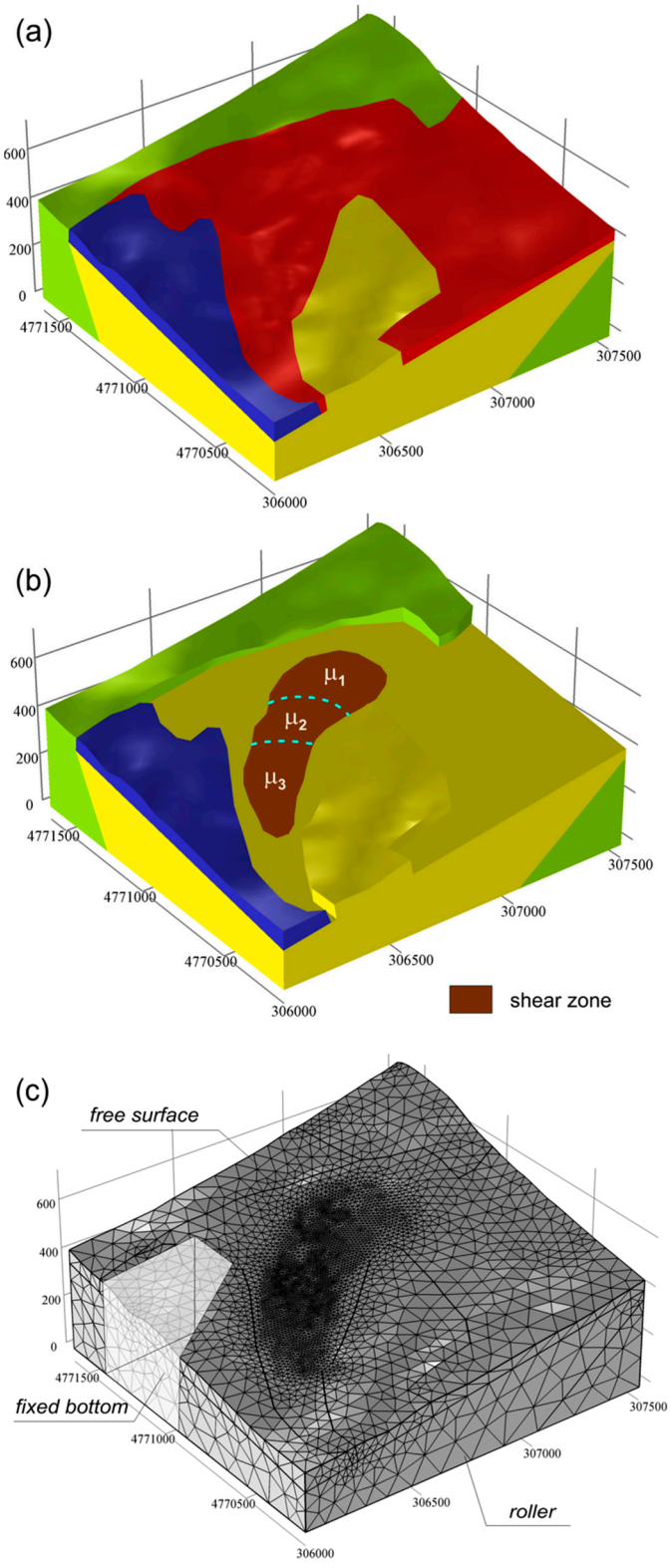

Figure 4. 3D FE Model: (**a**) Simplified geological model exploited in the FE environment; for each domain we report in Table 1 the physical and mechanical parameters relevant to the different lithologies, reported in Figure 2a; Panel (**b**) highlights the shear domain. The three sectors with different values of viscosity (μ) are also shown; the corresponding values are reported in Table 2; (**c**) Discretized numerical domain with the boundary conditions: fixed and roller ones.

Table 1. Input Parameters: Physical and Mechanical Properties of the Geo-Mechanical Units.

Rock Material	Density [kg/m^3]	Young's Modulus [MPa]	Poisson Ratio [–]	Viscosity [Pa·s]
Limestone bedrock	2200	8×10^3	0.28	1×10^{22}
Pelitic-Sandstone bedrock	1850	7×10^3	0.26	1×10^{21}
Debris deposit	1600	1×10	0.24	1×10^{18}
Colluvial deposit	1700	6×10	0.24	1×10^{20}
Shear band	1600	1×10	0.23	–

Table 2. Optimized Parameters. Physical Parameters Bounds Used for the Shear Band Sectors in the Optimization and the Best Estimated Value.

Viscosity [Pa·s]	Lower Bound	Upper Bound	Estimated Value
μ_1	1×10^{14}	5×10^{16}	5.3×10^{15}
μ_2	1×10^{12}	5×10^{14}	2.5×10^{13}
μ_3	1×10^{11}	5×10^{13}	1×10^{12}

We remark that such an accurate definition of the shear zone domain is not possible in the 2D scenario [8], that represents, for the lack of geometrical constraints along the considered section, a rougher model. However, it is worth noting that the proposed subdivision has no significant impact on the applicability of the method and a finer discretization, although involving an increase of the computational load, can be easily applied in more complex scenarios.

The 3D numerical domain is discretized by creating a mesh that consists of about 620,000 tetrahedral elements. The element sizes range from 2 to 200 m; moreover, a mesh refinement was applied within the shear-zone domain where higher deformation rates were expected. The generated mesh is then validated through several resolution tests [35,36], which indicate a negligible mesh-dependency of the solution, since the use of a finer mesh would have affected the results by less than 2%.

Regarding the boundary conditions, the upper part of the geometry model which represents the ground surface of the slope, is considered as unconstrained (free surface); the bottom boundary is fixed. The four lateral side boundaries are instead characterized by null horizontal displacement. Finally, the inner domain is characterized by continuity between the different geological units.

According to Griffiths and Lane [37], we perform our modeling in two stages: gravity loading, aimed at defining a stress field representative of the current stress state of the slope; landslide process, i.e., the kinematics simulation. During the gravity loading, the stress state of the slope is defined by considering the slope as subjected to the soil gravitational loads and assuming elastic soil behavior. At this level, only the generated stress field is considered while the nodal displacements are kept equal to zero. In the landslide process, the previously calculated stresses are applied to the whole domain and the Newtonian approach is considered to simulate the kinematical trend of the landslide during the 2009–2012 time interval. The analysis implicitly assumes that the landslide body, delimited by the underlying shear zone, is unstable or marginally stable: this is specifically verified by means of a limit equilibrium calculation that provided a stability factor of the landslide body close to unity. It is worthwhile stressing that for the considered Newtonian viscous flow, soil is assumed to behave as a single-phase material. As described before, this assumption is supported by the available open-pipe piezometric measurements (Supplementary Materials Figure S2), locally indicating moderate variations of the water level within the landslide debris and by electric piezometer measurements showing very low variations of the pore water pressure at the depth of the shear band. Accordingly, we can assume that the pore water pressure regime plays a minor role in the landslide evolution process and separation between pore fluid and soil skeleton behavior is not needed for the present study. Note that, in order to simulate the landslide debris movement approximately as a rigid body, in the considered physical context the viscosity values of the layers overlaying the shear domain (surrounding rocks) are chosen with different order of magnitude (Table 1).

In order to integrate all the available data described in Section 2 and solve the field Equation (1), the COMSOL Multiphysics finite-element modeling code is used.

The modelled displacement rates are evaluated at the topographic surface, projected along the satellite line of sight (LOS) and compared with the DInSAR measurements. In particular, the optimization procedure is performed by exploiting the CSK SBAS-DInSAR results (Figure 3). To detect the model providing the best agreement between DInSAR measurements and FE model, we use the Monte Carlo statistical method, which is based on the exploration of the parameter values in a defined space of variables (coordinate search method) [38,39]. This procedure allows us to find, for the three different shear band sectors, the viscosity parameters that correspond to the model that best-fits the DInSAR measurements. To evaluate the similarity between the data vs. model, we use the Root Mean Square Error (RMSE) cost function; it is represented by a weighted average of the residuals, expressed as:

$$RMSE = \sqrt{\frac{1}{N}\sum_{i}^{N}\frac{\left(d_{i,obs} - d_{i,mod}\right)^2}{\sigma_i}} \quad (2)$$

where $d_{i,obs}$ and $d_{i,mod}$ are the observed and modeled displacement of the $i^{-\text{th}}$ point, σ_i is the standard deviation for the N points.

4. Results

A quantitative comparison between the CSK SBAS-DInSAR measurements (Figure 5a) and the achieved model results projected along LOS (Figure 5b), computed in correspondence of the SAR coherent pixels is performed; the Figure 5c represents the difference (residuals) between data and model results. The residuals map (Figure 5c) shows the good fit between data and model results, revealed also by the RMSE value that is equal to 0.15 cm/yr, smaller than the accuracy of the SBAS-DInSAR measurements [28]. In addition, the performed analysis also provides a good temporal fit between the DInSAR deformation time series and the modeled one for the considered time interval (Supplementary Materials Figure S1).

Starting from the analysis that best-fits the displacement monitoring data, we evaluate the related viscosity parameters of the three sector of shear zone (μ_1, μ_2, μ_3). The corresponding estimated values are reported in Table 2, along with the initial ranges adopted for the analysis.

The optimized FE model allows for the analysis of the overall ground velocities field. In Figure 6a we show the amplitude and direction of the achieved velocity field; in this map the amplitude of the velocity field reaches a maximum value of 1.5 cm/yr at altitudes between 320 and 400 m a.s.l., in the middle-upper part of the unstable area. In addition, the model results well represent the slight curvature in the horizontal plane of the landslide process along the South-East direction, as also highlighted by the modeled vectors (Figure 6a). A comparative analysis between the morphological units of the Ivancich slope (ancient and active edges landslide) as proposed by Pontoni [23,24] and the model results are also reported (Figure 6b); more than the 70% of the mapped geomorphological structures (units 6–11) are enclosed in the region where the 2009–2012 deformation process is active. The units 12 and 13 are marginally involved while the units 1–4 seem to be not active in the considered time interval (with mean velocity lower than 0.3 cm/yr). Our analysis also highlights the existence of a spatially correlated deformation pattern (0.5 cm/yr) superimposed on the cataloged ancient structures located in the North Western region of the landslide slope.

Finally, we show a map with the computed shear rate values (Figure 7a) that represents the ratio of the shear stress to the dynamic viscosity. It is interesting to note that the landslide portions where the structures are damaged, as many photographs recorded in the Ivancich surroundings clearly show (Figure 7b), are in accordance with the distribution of the anomaly of the shear rate. In fact, serious damage corresponding to the P2, P3 and P5 sites are localized along the landslide boundaries and in correspondence of highest values of shear rate.

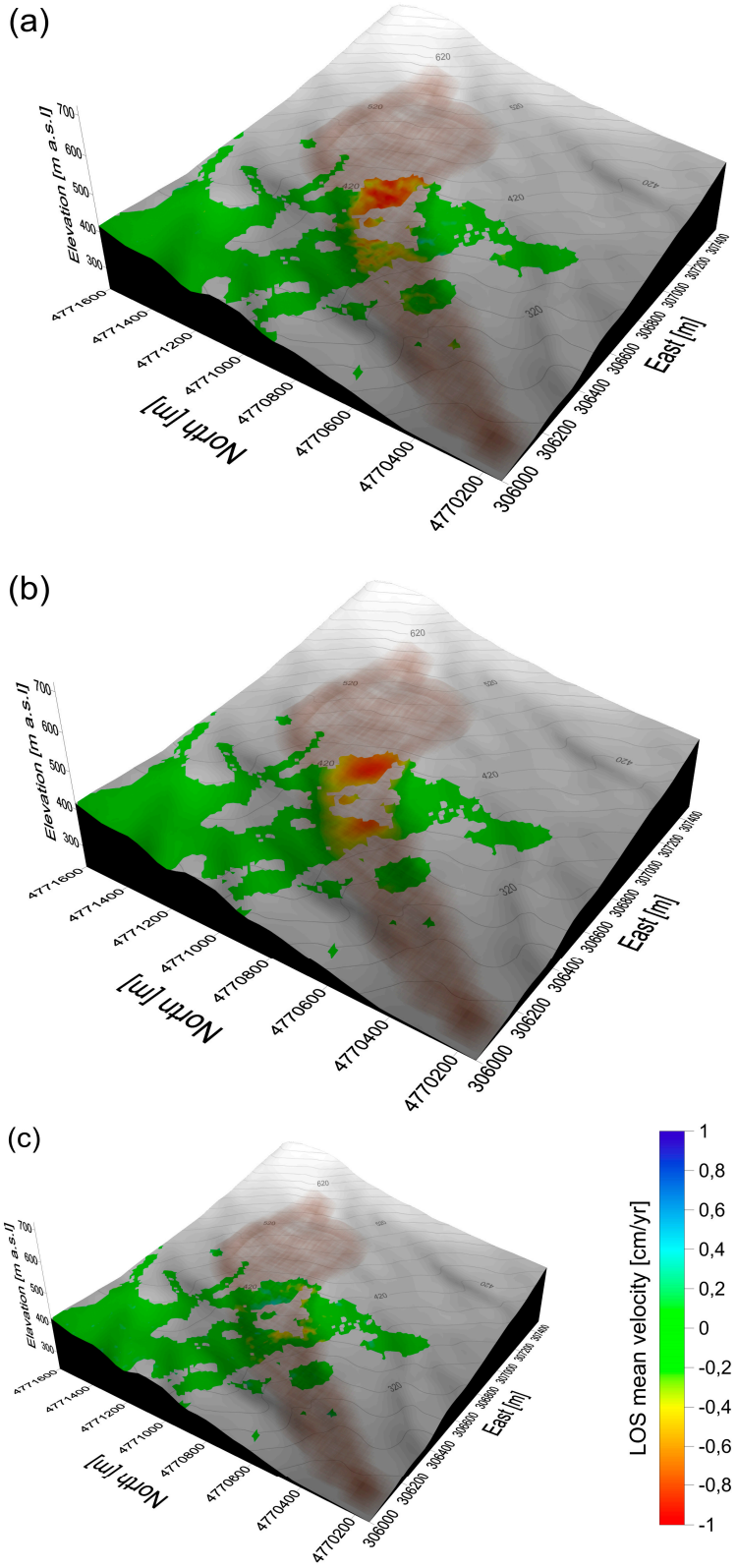

Figure 5. Geodetic inversion results: (**a**) Data; (**b**) Model and (**c**) Residuals relevant to the DInSAR velocity map superimposed on the filled contour DEM. The shading area indicates the unstable slope mass.

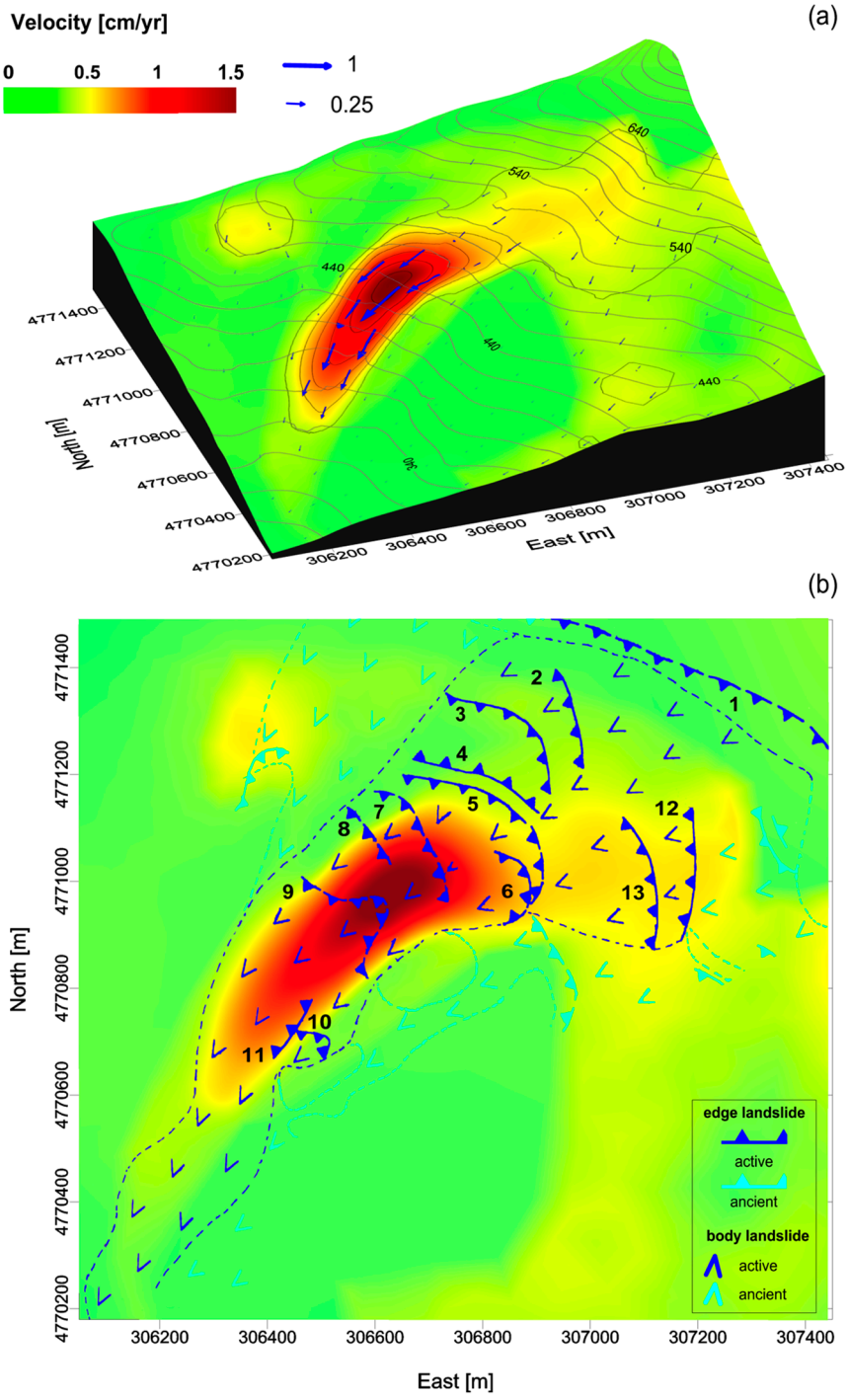

Figure 6. Analysis of FE Model results: (**a**) 3D view of modeled velocity vectors (blue arrows superimposed on the contour lines of the velocity field; (**b**) Modeled velocity map compared with the geomorphological evidences represented by the quiescent (cyan) and active (blue) elements as proposed by Pontoni [23,24].

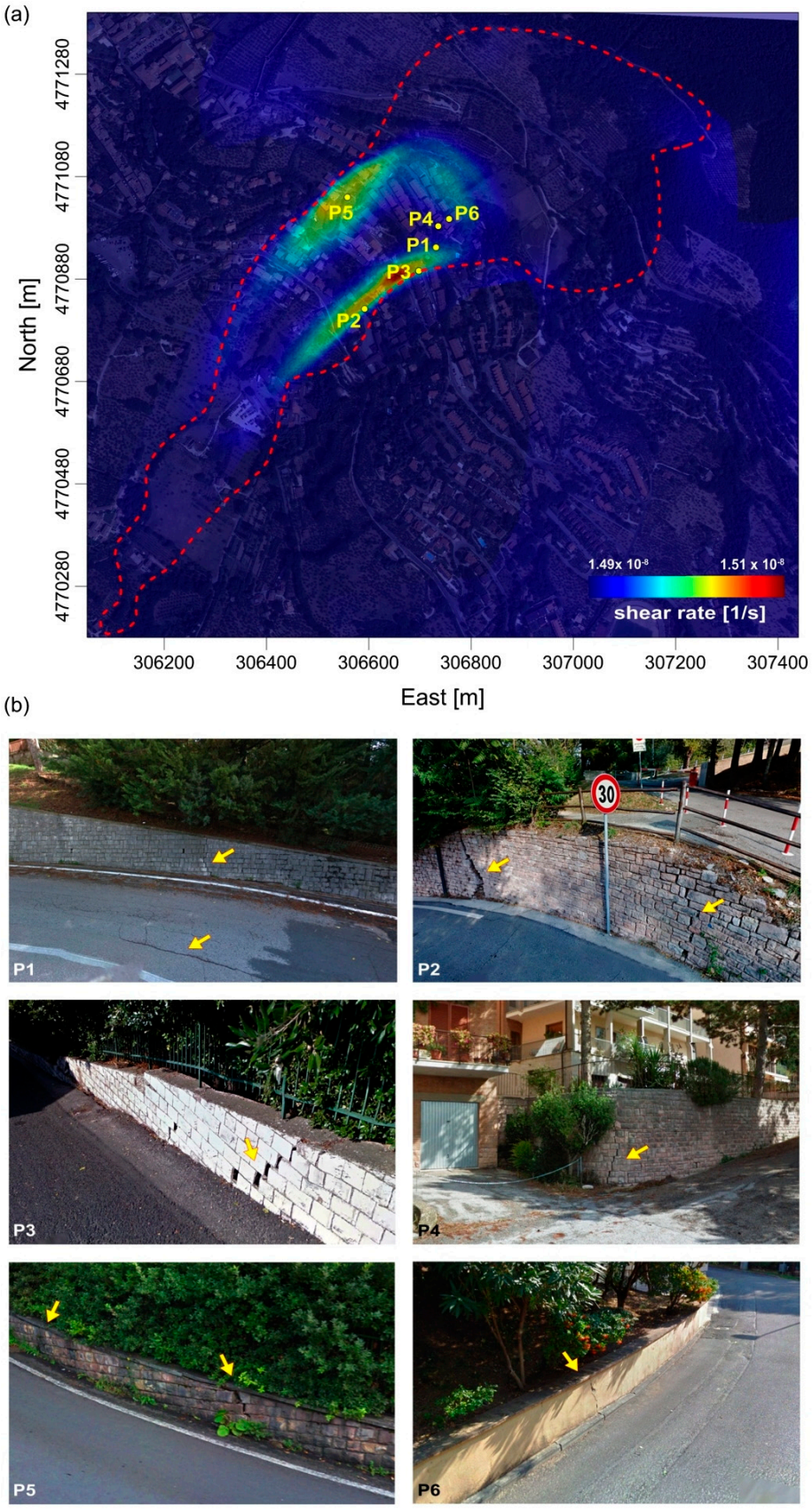

Figure 7. Shear rate map and structure damage: (**a**) Shear map superimposed on the satellite optical image of the Ivancich surrounding area (source Google Earth); (**b**) The pictures of the structure damage indicated with labels P1, P2, P3, P4, P5, P6 are shown.

5. Discussion

In this work, we perform a three-dimensional optimized model based on a fluid-dynamic physical scenario realizing an effective integration of satellite and terrestrial observations in the FE environment. In detail, based on the linearity of kinematics affecting the unstable mass as ensured by the DInSAR deformation time-series, we can assume the soil material behavior as Newtonian fluid, characterized by the viscosity parameter constant over time. Despite that, the Newtonian fluid assumption is not a rigorous constitutive model for the soil physical proprieties, it is useful to simulate the landslide kinematical behavior; we remark that this model can be applied only to a landslide-type where the shear zone geometry is well formed and well known by means of accurate and detailed in-situ investigations (Figure 2).

In this perspective, a three-dimensional kinematical model is performed, providing a full map of the current landslide velocities, both in terms of modules and corresponding directions. A spatial kinematic variability is also highlighted from the retrieved velocity map, since lower velocities are calculated along the lateral boundaries of the landslide with respect to the inner portions. The consistency of the model results with respect to the DInSAR velocity field (Figure 5) also represents a further back-validation of the 3D shear zone geometry. In addition, we compare the modeled velocity pattern with the main geomorphological features of the Ivancich slope (ancient and active edges landslide) highlighting a good match. In fact, the analysis reveals that more than the 70% of the mapped geomorphological structures are still active. The existence of a stable geological element made of in-place pelitic sandstone, along the left-hand side of the landslide at middle elevations, probably influences the direction of the phenomenon toward South-East, as supported by the geomorphological features of the study area (Figure 6). Moreover, we correlate the additional damage and the modeled shear rate. This study reveals that ruptures are most severe along the landslide boundaries between active and inactive sectors; this result is expected when the spatial gradient of the modeled velocities field in maximum (Figure 7). We argue that the information on the average landslide velocities and shear rate can provide an important contribution into predicting possible deformation scenarios for structures and infrastructures lying within the landslide area and for the land management of the whole area. Our results furnish a promising support for risk analysis of very slow landslides within a reasonable time span and for which the analysis can be considered as an expected representation of the coming years.

In order to show the advance of our 3D modeling respect to the 2D FE ones [8,18], we perform a comparative analysis between the retrieved velocity fields reported in Supplementary material (Figure S3). The achieved results point out a significant improvement of the residual values. It is worthwhile pointing out that the 3D optimized viscosity values are lower than those achieved via 2D modeling. These discrepancies could be related to: (i) the effect of the detailed shear zone geometry; (ii) a different confining effect and stress field of the three-dimensional model respect to the two-dimensional one. However, these results emphasize how the modeling approach is strongly influenced by the type of the performed dimensional analysis.

6. Conclusions

The achieved results clearly demonstrate how the integration of remote sensing, in-situ monitoring and FE modeling is strategic in performing detailed analyses of complex deformation scenarios. By benefiting from three-dimensional advanced modeling tools we can effectively investigate the overall mechanism of the evolution of the ground displacements related to slow landslide phenomena, as well as outline possible risk scenarios. As a matter of fact, if in-situ measurements or DInSAR-based analyses are capable of exploring the displacement trends of specific sectors of a landslide process, the three-dimensional model can provide a thorough physically-based conceptualization of the landslide kinematics, provided that the same model is calibrated and optimized against the aforementioned measurements.

The calibrated three-dimensional FE model provides more opportunities as a zonation tool capable of identifying and updating the status of the morphological structures originally mapped from in-situ investigations. The amplitude of the velocity field reaches a maximum value of 1.5 cm/yr at altitudes between 320 and 400 m a.s.l., in the middle-upper part of the unstable area; more than the 70% of the mapped geomorphological structures are enclosed in the region where the 2009–2012 deformation process is active. The model fully delineates the landslide portions that are subjected to different landslide velocities and this can be useful for land management purposes; therefore, the comparison between the 3D vs. 2D model results highlights that the sliding surface, calculated via the 3D geo-lithological model, is more realistic in respect to those realized in the 2D model.

Finally, we remark that the damage analysis detected in the Ivancich surroundings compared with the three-dimensional FE model results, reveals that ruptures are most severe along the boundary between active and inactive landslide sectors where the shear rate values are high. Hence, the proposed three-dimensional FE modeling tool represents a valuable support for landslide risk analyses and urban development planning within a specific territory area affected by complex slow-moving landslide processes.

Supplementary Materials: The following are available online at http://www.mdpi.com/2072-4292/8/8/670/s1. Figure S1: (**a**) CSK mean LOS velocity map superimposed on the 3D view of Satellite optical image with the DEM contour lines (grey lines). The shade of red shows the zone involved by the recent instability phenomenon. The blue triangles indicate the four SAR pixels of the CSK DInSAR measurements; (**b**) The plots allow comparing the time series of four SAR pixels (from upstream to downstream) and the fluid dynamic model projected in LOS. Figure S2: Limit Equilibrium (LE) analyses carried out in order to assess the stability conditions of the slope, based on the available geological, geomorphological and geotechnical dataset. In particular, a pore pressure distribution defined according to a finite element seepage analysis in agreement with the available piezometer measurements has been assigned in the LE calculation. According to the results of direct shear tests performed on samples taken at the depth of the sliding surface, a cohesion intercept equal to $c' = 0$ and a friction angle of $\varphi' = 15^{\circ}$ have been considered as operative values of the shear strength parameters along the shear band and have been used for the LE analysis. The calculation results indicate that the stability factor of a landslide body corresponding to the central portion of the examined landslide, i.e. the most active zone of the landslide area, is FS = 0.99, whereas FS is equal to 1.02 for the whole landslide body. This confirms that the whole landslide body is at LE conditions. Figure S3: (**a**) Modelled LOS velocity map. The black line shows the SS' trace, already presented in [18]; (**b**) Extrapolated profile along SS' from 3D model vs DInSAR measurements; (**c**) model and DInSAR measurements from [18]; (**d**) residuals comparison.

Acknowledgments: This work has been supported by EC FP7 LAMPRE project (contract No. 312384) and the Italian Department of Civil Protection. Part of the presented research has been carried out through the I-AMICA (Infrastructure of High Technology for Environmental and Climate Monitoring-PONa3_00363) project of Structural improvement financed under the National Operational Programme (NOP) for "Research and Competitiveness 2007–2013", co-funded with European Regional Development Fund (ERDF) and National resources. The Cosmo-SkyMed satellite images were acquired within the EC FP7 DORIS project (contract No. 242212). The Digital Elevation Model of the investigated zone was acquired through the SRTM archive.

Author Contributions: V.D.N., R.C., P.L. and P.T. conceived and organized the research activity. M.M. processed the SAR images and supervised the integration of the satellite measurements within the modeling procedure. R.C. and V.D.N. performed the optimization modeling procedure. P.T. supervised the research activity. All authors co-wrote the manuscript.

Conflicts of Interest: The authors declare no conflict of interest.

References

1. Herrera, G.; Fernandez-Merodo, J.A.; Mulas, J.; Pastor, M.; Luzi, G.; Moserrat, O. A landslide forecasting model using ground based SAR data: The Portalet case study. *Eng. Geol.* **2009**, *105*, 220–230. [CrossRef]
2. Manconi, A.; Casu, F.; Ardizzone, F.; Bonano, M.; Cardinali, M.; De Luca, C.; Gueguen, E.; Marchesini, I.; Parise, M.; Vennari, C.; et al. Brief Communication: Rapid mapping of landslide events: The 3 December 2013 Montescaglioso landslide, Italy. *Nat. Hazards Earth Syst. Sci.* **2014**, *14*, 1835–1841. [CrossRef]
3. Ranalli, M.; Gottardi, G.; Medina-Cetina, Z.; Nadim, F. Uncertainty quantification in the calibration of a dynamic viscoplastic model of slow slope movements. *Landslides* **2010**, *7*, 31–41. [CrossRef]
4. Comegna, L.; Picarelli, L.; Bucchignani, E.; Mercogliano, P. Potential effects of incoming climate changes on the behaviour of slow active landslides in Italy. *Landslides* **2013**, *13*, 373–391. [CrossRef]

5. Bernardie, S.; Desramaut, N.; Malet, J.-P.; Gourlay, M.; Grandjean, G. Prediction of changes in landslide rates induced by rainfall. *Landslides* **2015**, *12*, 481–494. [CrossRef]
6. Conte, E.; Donato, A.; Troncone, A. A finite element approach for the analysis of active slow-movine landslides. *Landslides* **2014**, *11*, 723–731. [CrossRef]
7. Fernández-Merodo, J.A.; García-Davalillo, J.C.; Herrera, G.; Mira, P.; Pastor, M. 2D viscoplastic finite element modeling of slow landslides: The Portalet case study (Spain). *Landslides* **2012**, *11*, 29–42. [CrossRef]
8. Castaldo, R.; Tizzani, P.; Lollino, P.; Calò, F.; Ardizzone, F.; Lanari, R.; Manunta, M. Landslide kinematical analysis through inverse numerical modeling and differential SAR interferometry. *Pure Appl. Geophys.* **2014**, *172*, 1–14.
9. Schädler, W.; Borgatti, L.; Corsini, A.; Meier, J.; Ronchetti, F.; Schanz, T. Geomechanical assessment of the Corvara earthflow through numerical modeling and inverse analysis. *Landslides* **2015**, *12*, 495–510.
10. Sansosti, E.; Casu, F.; Manzo, M.; Lanari, R. Space-borne radar interferometry techniques for the generation of deformation time series: An advanced tool for Earth's surface displacement analysis. *Geophys. Res. Lett.* **2010**, *37*, 1–9. [CrossRef]
11. Bovenga, F.; Wasowski, J.; Nitti, D.O.; Nutricato, R.; Chiaradia, M.T. Using COSMO/SkyMed X-band and ENVISAT C-band SAR interferometry for landslides analysis. *Remote Sens. Environ.* **2012**, *119*, 272–285. [CrossRef]
12. Colesanti, C.; Wasowsky, J. Investigating landslides with space-borne Synthetic Aperture Radar (SAR) interferometry. *Eng. Geol.* **2006**, *88*, 173–199. [CrossRef]
13. Herrera, G.; Gutiérrez, F.; García-Davalillo, J.C.; Guerrero, J.; Notti, D.; Galve, J.P.; Cooksley, G. Multi-sensor advanced DInSAR monitoring of very slow landslides: the Tena valley case study (central Spanish Pyrenees). *Remote Sens. Environ.* **2013**, *128*, 31–43. [CrossRef]
14. Usai, S. A least-squares database approach for SAR interferometric data. *IEEE Trans. Geosci. Remote Sens.* **2003**, *41*, 753–760. [CrossRef]
15. Ferretti, A.; Prati, C.; Rocca, F. Permanent Scatterers in SAR interferometry. *IEEE Trans. Geosci. Remote Sens.* **2001**, *39*, 8–20. [CrossRef]
16. Berardino, P.; Fornaro, G.; Lanari, R.; Sansosti, E. A new algorithm for surface deformation monitoring based on small baseline differential SAR interferograms. *IEEE Trans. Geosci. Remote Sens.* **2002**, *40*, 2375–2383. [CrossRef]
17. Lanari, R.; Mora, O.; Manunta, M.; Mallorqui, J.; Berardino, P.; Sansosti, E. A small baseline approach for investigating deformations on full resolution differential SAR interferograms. *IEEE Trans. Geosci. Remote Sens.* **2004**, *42*, 1377–1386. [CrossRef]
18. Calò, F.; Ardizzone, F.; Castaldo, R.; Lollino, P.; Tizzani, P.; Guzzetti, F.M. Manunta, Enhanced landslide investigations through advanced DInSAR techniques: The Ivancich case study, Assisi, Italy. *Remote Sens. Environ.* **2014**, *142*, 69–82. [CrossRef]
19. Cruden, D.M.; Varnes, D.J. Landslide types and processes. In *Landslides, Investigation and Mitigation*; Transportation Research Board Special Report 247; Turner, A.K., Schuster, R.L., Eds.; National Academy Press: Washington, DC, USA, 1996; pp. 36–75.
20. Angeli, M.G.; Pontoni, F. The innovative use of a large diameter microtunneling technique for the deep drainage of a great landslide in an inhabited area: The case of Assisi (Italy). In *Landslides in Research, Theory and Practice*; Thomas Telford Publisher: London, UK, 2000; pp. 1666–1672.
21. Canuti, P.; Marcucci, E.; Trastulli, S.; Ventura, P.; Vincenti, G. Studi per la stabilizzazione della frana di Assisi. In Proceedings of the National Geotechnical Congress, Bologna, Italy, 14–16 May 1986; Volume 1, pp. 165–174.
22. Felicioni, G.; Martini, E.; Ribaldi, C. *Studio dei Centri Abitati Instabili in Umbria*; Pubbl. n° 979 del CNR-GNDCI; Rubettino Publisher: Rome, Italy, 1996. (In Italian)
23. Pontoni, F. Geoequipe Studio Tecnico Associato Geologia–Ingegneria, Italy. Unpublished Technical Report, 1999. (In Italian).
24. Pontoni, F. Geoequipe Studio Tecnico Associato Geologia–Ingegneria, Italy. Unpublished Technical Report, 2011. (In Italian).
25. Fastellini, G.; Radicioni, F.; Stoppini, A. The Assisi landslide monitoring: A multi-year activity based on geomatic techniques. *Appl. Geomat.* **2011**, *3*, 91–100. [CrossRef]

26. Bovenga, F.; Nitti, D.O.; Fornaro, G.; Radicioni, F.; Stoppini, A.; Brigante, R. Using C/X-band SAR interferometry and GNSS measurements for the Assisi landslide analysis. *Int. J. Remote Sens.* **2013**, *34*, 4083–4104. [CrossRef]
27. Franceschetti, G.; Lanari, R. *Synthetic Aperture Radar Processing*; CRC Press: Boca Raton, FL, USA, 1999.
28. Bonano, M.; Manunta, M.; Pepe, A.; Paglia, L.; Lanari, R. From previous C-band to new X-band SAR systems: Assessment of the DInSAR mapping improvement for deformation time-series retrieval in urban areas. *IEEE Trans. Geosci. Remote Sens.* **2013**, *51*, 1973–1984. [CrossRef]
29. Arangio, S.; Calò, F.; di Mauro, M.; Bonano, M.; Marsella, M.; Manunta, M. An application of the SBAS-DInSAR technique for the assessment of structural damage in the city of Rome. *Struct. Infrastruct. Eng.* **2014**, *10*, 1–15. [CrossRef]
30. Guzzetti, F.; Manunta, M.; Ardizzone, F.; Pepe, A.; Cardinali, M.; Zeni, G.; Reichenbach, P.; Lanari, R. Analysis of ground deformation detected using the SBAS-DInSAR technique in Umbria, Central Italy. *Pure Appl. Geophys.* **2009**, *166*, 1425–1459. [CrossRef]
31. Manunta, M.; Marsella, M.; Zeni, G.; Sciotti, M.; Atzori, S.; Lanari, R. Two-scale surface deformation analysis using the SBAS-DInSAR technique: A case study of the city of Rome, Italy. *Int. J. Remote Sens.* **2008**, *29*, 1665–1684. [CrossRef]
32. Scifoni, S.; Bonano, M.; Marsella, M.; Sonnessa, A.; Tagliafierro, V.; Manunta, M.; Lanari, R.; Ojha, C.; Sciotti, M. On the joint exploitation of long-term DInSAR time series and geological information for the investigation of ground settlements in the town of Roma (Italy). *Remote Sens. Environ.* **2016**, *182*, 113–127. [CrossRef]
33. Notti, D.; Calò, F.; Cigna, F.; Manunta, M.; Herrera, G.; Berti, M.; Meisina, C.; Tapete, D.; Zucca, F. A user-oriented methodology for DInSAR time series analysis and interpretation: Landslides and subsidence case studies. *Pure Appl. Geophys.* **2015**, *172*, 3081–3105. [CrossRef]
34. Ranalli, G. *Rheology of the Earth*; Chapmann & Hall: London, UK, 1995.
35. Zienkiewicz, O.C.; Taylor, R.L. *The Finite Element Method: Basic Formulation and Linear Problems*; McGraw-Hill: Burlington, MA, USA, 1988; Volume 1.
36. Zhang, Z.; Zhu, J.Z. Analysis of the superconvergent patch recovery technique and a posteriori error estimator in the finite element method (II). *Comput. Methods Appl. Mech. Engrgy.* **1998**, *163*, 159–170. [CrossRef]
37. Griffiths, D.V.; Lane, P.A. Slope stability analysis by finite elements. *Geotechnique* **1999**, *49*, 387–403. [CrossRef]
38. Tarantola, A. *Inverse Problem Theory and Methods for Model Parameter Estimation*; Society for Industrial and Applied Mathematics (SIAM): Philadelphia, PA, USA, 2005; pp. 1–343.
39. Sen, M.K.; Stoffa, P.L. *Global Optimization Methods in Geophysical Inversion*; Cambridge University Press: Cambridge, UK, 2013.

© 2016 by the authors; licensee MDPI, Basel, Switzerland. This article is an open access article distributed under the terms and conditions of the Creative Commons Attribution (CC-BY) license (http://creativecommons.org/licenses/by/4.0/).